ORIGINAL ARTICLE

Analysis of the caudate artery with three-dimensional imaging

Yukio Oshiro, Ryoko Sasaki, Takaya Takeguchi, Kenji Ibukuro, Nobuhiro Ohkohchi

Y. Oshiro, R. Sasaki*, N. Ohkohchi
Department of Organ Transplantation Gastroenterological and Hepatobiliary Surgery, University of Tsukuba, Graduate School of Comprehensive Human Sciences, 1-1-1 Tennodai, Tsukuba, 305-8575, Japan

T. Takeguchi, K. Ibukuro
Department of Radiology, Mitsui Memorial Hospital, 1 Kandaizumityo, Tiyodaku, Tokyo, 101-8643, Japan

*Corresponding author:
Ryoko Sasaki, MD, PhD
Department of Organ Transplantation Gastroenterological and Hepatobiliary Surgery, University of Tsukuba, Graduate School of Comprehensive Human Sciences, 1-1-1 Tennodai, Tsukuba 305-8575, Japan
Tel ＋81-29-853-3221 Fax ＋81-29-853-3222
Email: rsasaki.dr@hotmail.co.jp

Key words: 3DCT; caudate lobe; caudate artery; communicating artery; hilar bile duct
Word Counts: 4043. Number of Figures: 5. Number of Tables: 4.

Abstract

Background/purpose To date there have been only a few radiological studies of the caudate artery. This study aimed to precisely analyze the caudate artery as well as the relationship between the caudate arteries, the arterial plexus at the hilar plate, and the hilar bile duct.

Methods Reconstructed three-dimensional (3D) images from 50 patients from CT during hepatic arteriography (CTHA) were analyzed. The caudate arteries were classified as right branches (I*r*s) or left branches (I*l*s). The communicating artery (CA) was defined as the artery connecting the right, left, segmental, and common hepatic arteries.

Results The caudate artery was divided into 3 types: an independent branch (Type 1); the common tract formed by I*r* and I*l* (Type 2); and an arterial branch from the CA (Type 3). The CA was recognized in 25 of 50 patients. There was a total of 65 arteries to the hilar bile duct observed in 40 patients, and 24 (37%) of these 65 arteries to the hilar bile duct originated from the caudate artery or CA.

Conclusion The caudate artery plays an important role not only in connecting the blood supply of the right and left livers but in the blood supply to the hilar bile duct.

Introduction

The caudate artery has been studied both anatomically and radiologically [1–10]. However, since it is not easily detected radiologically, there are relatively few studies of the caudate artery using radiological techniques [6–10]. Recent advances in multidetector-row computed tomography (MDCT) have made visualization of the entire small vascular system possible, allowing for the determination of the anatomy of small vessels. It has also become possible to reconstruct accurate and realistic 3D images at arbitrary angles [11, 12]. Furthermore, 3D imaging helps correlate preoperative and intraoperative findings by identifying reliable anatomic landmarks [13, 14]. Among many imaging modalities, CTHA is the most sensitive for detecting the caudate artery. Moreover, CTHA can provide precise information about the relationship between tiny vessels and adjacent structures.

HCC in the caudate lobe is difficult to treat due to its anatomical features. Recently, however, resection of the caudate lobe has been carried out safely due to advances in surgical technique. Therefore, it is useful for surgeons to be familiar with the precise anatomy of the caudate lobe. Nevertheless, among most medical facilities in Japan, TACE still plays a major role in the treatment of caudate HCC. Approximately 16–31% of caudate HCCs are fed by multiple arterial branches arising from different origins [2, 7–9]. Knowledge of the precise anatomy is important for TACE as well as surgery [15].

Methods

Patients

Between September 2004 and October 2008, 150 patients with hepatic tumors detected by ultrasound examination underwent CTHA as well as CT during arterial portography (CTAP) for preoperative evaluation, TACE, or radiofrequency ablation (RFA). Out of 150 patients, 93 patients were randomly selected for 3D image reconstruction, but 43 of 93 patients were eliminated from the analysis due to tumors adjacent to the caudate lobe, insufficient or excessive contrast enhancement, status post- right or left hepatectomy, or hepatic arterioportal shunt. The 50 analyzed patients had no abnormal lesions in the caudate lobe and hepatic hilum and sufficient contrast medium in the hepatic artery for visualization. The 50 patients consisted of 33 men and 17 women with a median age of 70 years (range, 45 to 83 years).

Imaging

All studies were performed by using a 64-slice (32-detector) MDCT scanner (Sensation Cardiac, Siemens, Forchheim, Germany). When obtaining digital subtraction angiograms for preoperative evaluation or TACE, we placed a catheter in the common hepatic artery (CHA) or proper hepatic artery (PHA). For CTHA, 35 ml of contrast material (150 mg of iodine per ml; Iopamidol 150; Schering, Berlin, Germany) was injected at a rate of 1.5 ml/sec. Data acquisition started 20 seconds after the initiation of contrast injection. All images were obtained with 0.6 mm collimation, 1.2 pitch, 120 kV, 230 mA, and 0.5 sec rotation time. The axial images were reconstructed with a 512 × 512 matrix, at 1-mm thickness intervals. The 2D CT images were transferred to the workstation (SYNAPSE VINCENT: Fujifilm Medical, Tokyo, Japan), and one of the authors (Y. O.) generated the 3D images. Reconstructed 3D images were independently evaluated by 3 radiologists (K.I., T.T., and K.N.) to confirm that the images were appropriate for analyzing the caudate arteries and CA.

Definition of the caudate lobe, caudate artery, and CA

The caudate lobe is an independent hepatic lobe that does not belong to either the right or left hepatic lobe. In 1953, the caudate lobe was anatomically divided into 3 parts [16]: the right portion, the left portion, and the caudate process. Likewise, in 1985, Kumon also divided the caudate lobe into 3 parts: Spiegel lobe, the caudate process, and the paracaval portion, [17]. According to this definition of the caudate lobe and the classification of Kumon [17], we defined the right branch (I*r*) as the branch to the right part of the caudate lobe (the caudate process and the paracaval portion) and the left branch (I*l*) as the branch to the left part of the caudate lobe (Spiegel lobe). Additionally, we defined the CA as the artery connecting the right hepatic artery (RHA), left hepatic artery (LHA), segmental hepatic artery, and CHA.

Results

Arterial supply to the caudate lobe

On average, there were 1.1 ± 0.8 (range, 0 to 3) I*r* and 1.5 ± 0.7 (range, 1 to 4) I*l* arteries (n = 50).

Three variations of the caudate artery

The caudate artery arose in 3 general types (Figure 1). In Type 1, the caudate artery was an independent branch of the hepatic artery supplying the caudate lobe. In Type 2, the caudate artery was a common trunk originating from the hepatic artery that gave off I*r* and I*l* branches. In Type 3, the caudate artery was a branch from the CA. The branching patterns in 50 patients were as follows: 15 (30%) were Type 1, 6 (12%) were Type 2, 17 (34%) were Type 3, 4 (8%) were Type 1 + Type 2, and 8 (16%) were Type 1 + Type 3 (Table 1). The combination of the caudate artery of the 50 patients is shown in each patient in Table 2.

Type 1: Independent caudate artery and its origin

There were 47 independent caudate arteries (22 I*r*s and 25 I*l*s) seen in 27 of 50 patients (Table 3). I*r*s originated from the right posterior segmental artery (Post. A) (11 of 22 I*r*s; 50%), RHA (7 of 22 I*r*s; 32%), right anterior segmental artery (Ant. A) (3 of 22 I*r*s; 14%), and middle hepatic artery (MHA) (1 of 22 I*r*s; 4%). The origins of the I*l*s included the LHA (13 of 25 I*l*s; 52%), Post. A (5 of 25 I*l*s; 20%), MHA (4 of 25 I*l*s; 16%), and RHA (3 of 25 I*l*s; 12%). An example of a Type 1 caudate artery is shown in Figure 3.

Type 2: Common trunk formed by both I*r* and I*l* and its origin

A common trunk formed by I*r* and I*l* was seen in 10 of 50 patients (Table 3). The common trunk arose from the LHA in 4 patients (40%), Post. A in 2 patients (20%), RHA in 2 patients (20%), Ant. A in 1 patient (10%), and MHA in 1 patient (10%). An example of a Type 2 caudate artery is shown in Figure 4.

Patterns of CA

A Type 3 caudate artery was seen in 25 of 50 patients (Table 1). Since 1 patient had 2 CAs, the total number of CA was 26. The configurations of the CA were divided into 4 groups (Figure 2). Nine (35%) of 26 were classified as Group 1 (between RHA and LHA).

Three (12%) of 26 were classified as Group 2 (between Post. A, RHA, and LHA). Three (12%) of 26 were classified as Group 3 (between Post. A and LHA). Eleven (42%) of 26 were classified as Group 4 (other). Each CA gave off 1 to 4 caudate arteries.

Type 3: Caudate artery arising from the CA and its origin (**Table 2**)

The 17 patients of the Type 3 are broken down as follows, Group 1: 1I*r*, 1I*l*, 2 patients; 1I*r*, 2I*l*s, 2 patients; 1I*r*, 3I*l*s, 1 patient; 2I*r*s, 2I*l*s, 1 patient. Group 2: 1I*r*, 1I*l*, 1 patient; 2I*l*s 1 patient. Group 3: 1I*r*, 1I*l*, 2 patients. Group 4: 1I*r*, 2I*l*s, 4 patients; 1I*r*, 1I*l*, 1 patient; 2I*r*s, 2I*l*s, 1 patient; 3I*l*s, 1 patient. The 8 patients of the Type 1+3 are broken down as follows. Post. A(3I*r*s)+CA(Group1; 4I*l*s) 1 patient; RHA(1I*r*)+CA(Group 1; 2I*l*s) 1 patient; Ant. A(1I*r*)+CA(Group 1; I*r*, I*l*) +CA(Group 3; I*r*, I*l*) 1 patient; Ant. A(1I*r*)+CA(Group 2; 1I*l*), 1 patient; Post. A(1I*r*)+CA(Group 4; 1I*r*, 2I*l*s) 1patient; LHA(1I*l*)+CA(Group 4; 1I*r*, 1I*l*) 1patient; LHA(1I*l*)+CA(Group 4; 1I*r*) 1patient; MHA(1I*r*) +CA(Group 4; 1I*r*, 1I*l*) 1patient. An example of a Type 3 caudate artery is shown in Figure 5.

Artery supplying the hilar bile duct and its origin

The artery supplying the hilar bile duct was observed in 40 of 50 patients (Table 4). The arterial supply was detected by an enhancement in the wall of the hilar bile duct. Additionally, when an artery is attached to the enhanced hilar bile duct, we considered it to be the artery supplying the hilar bile duct. Arteries in the 3 o'clock and 9 o'clock positions close to the hilar bile duct were detected in 22 patients (55%) and in 25 patients (63%), respectively. Most 3 o'clock (13/22, 59%) and 9 o'clock arteries (19/25, 76%) originated from the RHA. The rest of the 3 o'clock and 9 o'clock arteries arose from the Post. A, LHA, CA, I*r*, or I*l*. When the wall in the hilar bile duct was enhanced without the presence of both 3 and 9 o'clock arteries, the arterial supply was considered to originate from the peribiliary plexus. In the 18 patients where the hilar bile duct was supplied by the peribiliary plexus, the hilar bile duct with wall enhancement was located close to the CA (6/18), I*r* (4/18), I*l* (3/18), common trunk (2/18), MHA (2/18), and LHA (1/18). In short, a total of 15 (83%) in 18 peribiliary plexuses originated from the caudate artery or the CA. An example of Type 3 caudate arteries and 3 and 9 o'clock arteries arising from the CA is shown in Figure 5.

Discussion

MDCT with 3D imaging has the ability to demonstrate complex anatomic relationships in hepatobiliary disease that are difficult to appreciate with 2D axial images [13, 14, 18, 19]. To our knowledge, this is the first study to retrospectively analyze the origin and course of the caudate artery using 3D images reconstructed from CTHA.

In this study, we originally classified the origin of the caudate artery (Figure 1). Stapleton *et al.* [3] described that the caudate lobe received branches from both the right and left hepatic arteries but the patterns were different in each subject. Two main patterns were recognized, a ‘tree’ pattern and an ‘arcade’ pattern. In the tree pattern, the caudate lobe was supplied by a single main artery arising centrally, either from the proximal RHA or the LHA. In the arcade pattern, the caudate lobe arterial supply consisted of an artery that ran along the cranial aspect of the hepatic duct confluence and represented a fusion of similarly-sized vessels arising from the distal LHA and RHA. In our study, accordingly to the classification proposed by Stapleton *et al.* [3], the independent branch (Type 1) and the common trunk (Type 2) might be consistent with the tree pattern, while the branch from CA (Type 3) might be consistent with the arcade pattern.

There have been several studies that have focused on the arterial supply to the hilar bile duct that is closely associated with the caudate artery and CA in the hilar plate [3, 4, 18, 20]. Vellar [4] described, with injection studies, that the hilar arterial plexus is not only involved in the blood supply of the confluence of the bile ducts but also the most important collateral between the RHA and LHA. In addition, the majority of branches to the hilar plate plexus originated from the RHA and LHA supplied the caudate lobe. Similarly, in our 25 of 50 cases, several arteries arising from the RHA, LHA, and segmental hepatic artery connected to each other in the hilar plate, supplied the hilar bile duct, and also gave off branches supplying the caudate lobe. Therefore, the vessel we called the CA in our study was the equivalent of a major artery in the arterial plexus in previous studies.

Biliary complication rates of up to 34% remain a serious problem in living-related liver transplantation; ischemia of the biliary tract is the most important factor contributing to biliary strictures or anastomotic leakage [3]. Histologic examination of the failed duct-to-duct reconstructions often showed the loss of the 3 o'clock and 9 o'clock arteries on the recipient side [21]. However, methods to preserve the blood supply of the donor graft bile duct are less clear. Gunji *et al.* [22] stated that division of the origin of the CA during graft donation might lead to biliary ischemia. We agree with their suggestion because, in our findings, the origin of the CA and the caudate artery certainly were near the proximal RHA, LHA, and segmental hepatic arteries in the hilar plate.

Although HCC arising in the caudate lobe is difficult to treat, TACE potentially improves the prognosis of caudate HCC [8]. 16–31% of caudate HCCs are fed by multiple arterial branches arising from different origins[2, 7–9]. These factors might make it more difficult to control caudate HCC using TACE. Therefore we consider that knowledge of the precise anatomy of the caudate artery may be helpful for the effective TACE. In contrast, it has been reported that the incidence of main bile duct necrosis by selective TACE of A1, A4 was approximately 6% [23]. The reason why bile duct complications occur after TACE is that the biliary tree is supplied primarily by arterial blood alone [24]. When embolic materials are injected into a tumor-feeding caudate artery, they may flow into another vessel supplying the bile duct through the CA. As supporting evidence, our findings indicated that the CA and the caudate artery, such as I*r*, I*l*, and the common trunk, supply the hilar bile duct. We should recognize the arterial network in the hilar plate and take care injecting embolic materials into the artery supplying the bile duct when performing the TACE. As a result, we may be able to prevent the bile duct ischemia and necrosis. This is an important point that we must keep in mind.

Tohma *et al.* [20] clarified, in evaluations with CT and angiography during temporary balloon occlusion of the RHA or LHA, that the communicating arterial arcade was consistently present in the hilar plate. The communicating arterial arcade has been recognized as one of the most important collateral pathways into the liver [15, 16, 20]. From the report of Miyazaki *et al.* [25], when the interlobar hepatic artery running into the Glissonian sheath around the hepatic duct confluence is preserved, one major lobar branch of the hepatic artery involved by tumor invasion could be safely resected without reconstruction. The interlobar hepatic artery referred to in this report corresponds to the CA in our study. Therefore, the recognition of the arterial network in the hilar plate helps not only in reducing intraoperative bleeding but also in performing successful surgery for extrahepatic cholangiocarcinoma without inducing postoperative hepatic failure.

Several limitations of this study need to be addressed. One potential weakness of this study is that there was a possibility of missing some small caudate arteries because not all of the caudate arteries could be visualized by CTHA in each patient. This study is also limited by the small number of patients. The results of our study will need to be confirmed in studies with more patients.

Conclusions

In conclusion, 3D imaging reconstructed by CTHA showed that the caudate artery plays an important role not only in the arterial collateral system of the liver but also in the blood supply to the hilar bile duct. The recognition of this vascular anatomy is clinically useful for performing liver resection for extrahepatic cholangiocarcinoma, living-related liver transplantation, and effective TACE for HCC.

Acknowledgement

The authors thank Dr. M. Ryu for his valuable comments and suggestions on this paper. The authors also thank Mr. K. Kotera and Ms. K. Suzuki of Fujifilm Medical Co., Ltd, for their kind support in performing this clinical research, and Dr. K. Nasu for his sincere corporation in evaluating this new imaging analysis.

Conflict of interest statement No conflict of interest

References

1. Michels NA. Blood supply of the caudate and the quadrate lobes. In: Michels NA, editors. Blood supply and anatomy of the upper abdominal organs with descriptive atlas. Philadelphia: JB Lippincott; 1955. p. 147-8.
2. Mizumoto R, Suzuki H. Surgical anatomy of the hepatic hilum with special reference to the caudate lobe. World J Surg. 1988; 12:2-10.
3. Stapleton GN, Hickman R, Terblanche J. Blood supply of the right and left hepatic duct. Br J Surg. 1998; 85:202-7.
4. Vellar ID. The blood supply of the biliary ductal system and its relevance to vasculobiliary injures following cholecystectomy. Aust NZ Surg. 1999; 69:816-20.
5. Lee UY, Murakami G, Han SH. Arterial supply and biliary drainage of the dorsal liver: a dissection study using controlled specimens. Anat Sci Int. 2004; 79:158-66.
6. Lunderquist A. Arterial segmental supply of the liver. Acta Radiol Diagn (Stockh). 1967; 272:5-86.
7. Miyayama S, Matsui O, Kameyama T, Hirose J, Konishi H, Chyotoh S, et al. Angiographic anatomy of arterial branches to the caudate lobe of the liver, with special reference to its effect on transarterial embolization for hepatocellular carcinoma. Jpn J Clin Radiol. 1990; 35:353-9. (in Japanese)
8. Terayama N, Miyayama S, Tatsu H, Yamamoto T, Toya D, Tanaka N, et al. Subsegmental transcatheter arterial embolization for hepatocellular carcinoma in the caudate lobe. J Vasc Interv Radiol. 1988; 9:501-8.
9. Yoon CJ, Chung JW, Cho BH, Jae HJ, Kang SG, Kim HC, et al. Hepatocellular carcinoma in the caudate lobe of the liver: angiographic analysis of tumor-feeding arteries according to subsegmental location. J Vasc Interv Radiol. 2008; 19:1543-50.
10. Miyayama S, Yamashiro M, Hattori Y, Orito N, Matsui K, Tsuji K, et al. Angiographic Evaluation of Feeding Arteries of Hepatocellular Carcinoma in the Caudate Lobe of the Liver. Cardiovasc Intervent Radiol. 2011; 34:1244-53.
11. Takahashi K, Sasaki R, Kondo T, Oda T, Murata S, Ohkohchi N. Preoperative 3D volumetric analysis for liver congestion applied in a patient with hilar

cholangiocarcinoma. Langenbecks Arch Surg. 2010; 395:761-5.

12. Shinohara Y, Ryu M. Demonstration of the hilar biliary confluence using 3D computed tomography. Semin Intervent Radiol. 1995; 12:138-45.
13. Endo I, Shimada H, Sugita M, Fujii Y, Morioka D, Takeda K, et al. Role of three-dimensional imaging in operative planning for hilar cholangiocarcinoma. Surgery. 2007; 142:666-75.
14. Sasaki R, Kondo T, Oda T, Murata S, Wakabayashi G, Ohkohchi N, et al. Impact of three-dimensional analysis of multidetector row computed tomography cholangioportography in operative planning for hilar cholangiocarcinoma. Am J Surg. 2011; 202:441- 8.
15. Ibukuro K, Tsukiyama T, Mori K, Inoue Y. The congenital anastomoses between hepatic arteries: angiographic appearance. Surg Radiol Anat. 2000; 22:41-5.
16. Healy JE Jr, Schroy PC. Anatomy of the biliary ducts within the human liver; analysis of the prevailing pattern of branchings and the major variations of the biliary ducts. AMA Arch. Surg. 1953; 66:599-616.
17. Kumon M. Anatomy of the caudate lobe with special reference to portal vein and bile duct. Acta Hepatol Jpn. 1985; 26:1193-9.
18. Lee MG, Park KB, Shin YM, Yoon HK, Sung KB, Kim MH, et al. Preoperative evaluation of hilar cholangiocarcinoma with contrast-enhanced three-dimensional fast imaging with steady-state precession magnetic resonance angiography: comparison with intraarterial digital subtraction angiography. World J Surg. 2003; 27:278-83.
19. Cho A, Okazumi S, Takayama W, Takeda A, Iwasaki K, Sasagawa S, et al. Anatomy of the right anterosuperior area of the liver: evaluation with helical CT during arterial portography. Radiology. 2000; 214:491-5.
20. Tohma T, Cho A, Okazumi S, Makino H, Shuto K, Mochiduki R, et al. Communicating arcade between the right and left hepatic arteries: evaluation with CT and angiography during temporary balloon occlusion of the right or left hepatic artery. Radiology. 2005; 237:361-5.

21. Kasahara M, Egawa H, Takada Y, Oike F, Sakamoto S, Kiuchi T, et al. Biliary reconstruction in right lobe living-donor liver transplantation: Comparison of different techniques in 321 recipients. Ann Surg. 2006; 243:559-66.
22. Gunji H, Cho A, Tohma T, Okazumi S, Makino H, Shuto K, et al. The blood supply of the hilar bile duct and its relationship to the communicating arcade located between the right and left hepatic arteries. Am J Surg. 2006; 10:161-5.
23. Miyayama S, Yamashiro M, Okuda M, Yoshie Y, Nakashima Y, Ikeno H,et al. Main bile duct stricture occurring after transcatheter arterial chemoembolization for hepatocellular carcinoma. Cardiovasc Intervent Radiol. 2010; 33:1168-79.
24. Kobayashi S, Nakanuma Y, Terada T, Matsui O. Postmortem survey of bile duct necrosis and biloma in hepatocellular carcinoma after transcatheter arterial chemoembolization therapy: relevance to microvascular damages of peribiliary capillary plexus. Am J Gastroenterol. 1993; 88:1410-5.
25. Miyazaki M, Ito H, Nakagawa K, Ambiru S, Shimizu H, Yoshidome H, et al. Unilateral hepatic arterial reconstruction is unnecessary in biliary tract carcinomas involving lobar hepatic artery: implications of interlobar hepatic artery and its preservation. Hepatogastroenterology. 2000; 47:1526-30.

FIGURE LEGENDS

Fig. 1

The caudate artery arose in 3 general patterns. The caudate artery was found to be either an independent arterial branch (Type 1), a common trunk that branched into a right caudate artery (I*r*) and a left caudate artery (I*l*) (Type 2), or an arterial branch arising from communicating artery (CA) (solid black line) (Type 3). RHA = right hepatic artery, MHA = middle hepatic artery, LHA = left hepatic artery

Fig. 2

Communicating patterns of the communicating artery (CA) (solid black line) were divided into 4 groups. CAs between the right hepatic artery (RHA) and left hepatic artery (LHA) were classified as Group 1. CAs between the right posterior segmental artery (Post. A), RHA, and LHA were classified as Group 2. CAs between the Post. A and LHA were classified as Group 3. CAs between other arteries were classified as Group 4. MHA = middle hepatic artery

Fig. 3

CTHA shows that the left caudate artery (I*l*) arose independently from the left hepatic artery (LHA). X is the origin of I*l* (A) (B). Three-dimensional imaging helps clarify the structure of the Type 1 caudate artery and its origin. X is the origin of I*l* (C) (D). RHA = right hepatic artery, MHA = middle hepatic artery, PHA = proper hepatic artery

Fig. 4

CTHA shows that the common trunk which branches into the right caudate artery (I*r*) and the left caudate artery (I*l*) arises from the right anterior segmental artery (Ant. A). X is the origin of the common trunk of I*r* and I*l* (A). Three-dimensional imaging helps clarify the origin and course of the Type 2 caudate artery. X is the origin of the common trunk (D). Post. A = right posterior segmental artery, MHA = middle hepatic artery, LHA = left hepatic artery, PHA = proper hepatic artery, RHA= right hepatic artery

Fig. 5

CTHA shows that the communicating artery (CA) was located between the right posterior segmental artery (Post. A), middle hepatic artery (MHA), and left hepatic artery (LHA), cranial to the portal bifurcation, and close to the hilar bile duct (BD). In this patient, the CA was classified as Group 4. Two left caudate arteries (I*l*s) arose from the CA. X1 and X2 are the origins of the I*l*s, respectively. Y1 is the origin of the CA arising from the LHA. Y2 is the origin of the CA arising from the Post. A. Y3 is the origin of the CA arising from the MHA. Z is the junction where the CA arises from the LHA, the Post. A, and the MHA (A)

(B) (C) (D). Three-dimensional imaging yields precise information on the structure of the portal vein, hilar BD, Type 3 caudate artery, CA between the Post. A, MHA, and LHA as well as the origins of the CA and the Type 3 caudate artery (E) (F).

Table 4. Number of arteries supplying the hilar bile duct and their origins (40/50 patients)

Artery supplying the hilar bile duct	No. of arteries	Origin									
		Post. A	Ant. A	RHA	MHA	LHA	CA	I*r*	I*l*	common	unknown
3 o'clock artery	22	0	0	13	0	2	4	1	1	0	1
9 o'clock artery	25	1	0	19	0	1	3	0	0	0	1
Peribiliary plexus	18	0	0	0	2	1	6	4	3	2	0
Total	65	1	0	32	2	4	13	5	4	2	2

Post. A, right posterior segmental artery; Ant. A, right anterior segmental artery; RHA, right hepatic artery; MHA, middle hepatic artery; LHA, left hepatic artery; CA, communicating artery; I*r*, right caudate artery; I*l*, left caudate artery; common, common trunk formed by I*r* and I*l*

Table 1. Branching patterns of the caudate artery

No. of patients	**Type 1 (%)**	**Type 2 (%)**	**Type 3 (%)**	**Type 1 + Type 2 (%)**	**Type 1 + Type 3 (%)**
50	15 (30%)	6 (12%)	17 (34%)	4 (8%)	8 (16%)

Table 2. The combination of the caudate artery in 50 patients

	Combination	Number of patients
Type 1 15 patients	Post. A(1I*r*)+LHA(1I*l*)	3
	LHA(1I*l*)	3
	Post. A(1I*r*)+RHA(1I*l*)	2
	RHA(1I*l*)+LHA(1I*l*)	1
	RHA(2I*r*s)+LHA(I*l*)	1
	RHA(2I*r*s)+MHA(2I*l*s)	1
	RHA(1I*r*, 1I*l*)	1
	MHA(1I*l*)	1
	Post. A(2I*l*s)	1
	Post. A(3I*l*s)	1
Type 2 6 patients	RHA (common; 1I*r*, 3I*l*s)	1
	RHA (common; 1I*r*, 1I*l*)	1
	Post. A (common; 1I*r*, 3I*l*s)	1
	MHA (common; 2I*r*s, 2I*l*s)	1
	LHA (common; 2I*r*s, 2I*l*s)	1
	LHA (common; 1I*r*, 1I*l*)	1
Type 3 17 patients	Group 1	
	1I*r*, 1I*l*	2
	1I*r*, 2I*l*s	2
	1I*r*, 3I*l*s	1
	2I*r*s, 2I*l*s	1
	Group 2	
	1I*r*, 1I*l*	1
	2I*l*s	1
	Group 3	
	1I*r*, 1I*l*	2
	Group 4	
	1I*r*, 2I*l*s	4
	1I*r*, 1I*l*	1
	2I*r*s, 2I*l*s	1
	3I*l*s	1

Type 1+Type2 4 patients	Post. A(1I*r*)+LHA(common; 1I*r*, 2I*l*s)	1
	RHA(1I*r*)+LHA(common; 1I*r*, 1I*l*)	1
	LHA(1I*l*)+Post.A(common; 1I*r*, 1I*l*)	1
	LHA(1I*l*)+Ant. A(common; 1I*r*, 1I*l*)	1
Type 1+Type3 8 patients	Post. A(3I*r*s)+CA(Group 1; 4I*l*s)	1
	RHA(1I*r*)+CA(Group 1; 2I*l*s)	1
	Ant. A(1I*r*)+CA(Group 1;I*r*, I*l*) +CA(Group 3;I*r*, I*l*)	1
	Ant. A(1I*r*)+CA(Group 2; 1I*l*)	1
	Post. A(1I*r*)+CA(Group 4; 1I*r*, 2I*l*s)	1
	LHA(1I*l*)+CA(Group 4; 1I*r*, 1I*l*)	1
	LHA(1I*l*)+CA(Group 4; 1I*r*)	1
	MHA(1I*r*) +CA(Group 4; 1I*r*, 1I*l*)	1

Post. A, right posterior segmental artery; I*r*, right caudate artery; LHA, left hepatic artery; I*l*, left caudate artery; RHA, right hepatic artery; MHA, middle hepatic artery; common, common trunk formed by I*r* and I*l*; Ant. A, right anterior segmental artery; CA, communicating artery

Table 3. Number of independent caudate arteries (Type 1) and common trunks formed by I*r* and I*l* (Type 2) and their origins

Caudate artery	**n**	**Origin**				
		Post. A (%)	**Ant. A (%)**	**RHA (%)**	**MHA (%)**	**LHA (%)**
Type 1 Total	47	16 (34%)	3 (6%)	10 (21%)	5 (11%)	13 (28%)
I*r*	22	11 (50%)	3 (14%)	7 (32%)	1 (4%)	0
I*l*	25	5 (20%)	0	3 (12%)	4 (16%)	13 (52%)
Type 2	10	2 (20%)	1 (10%)	2 (20%)	1 (10%)	4 (40%)

Post. A, right posterior segmental artery; Ant. A, right anterior segmental artery; RHA, right hepatic artery; MHA, middle hepatic artery; LHA, left hepatic artery

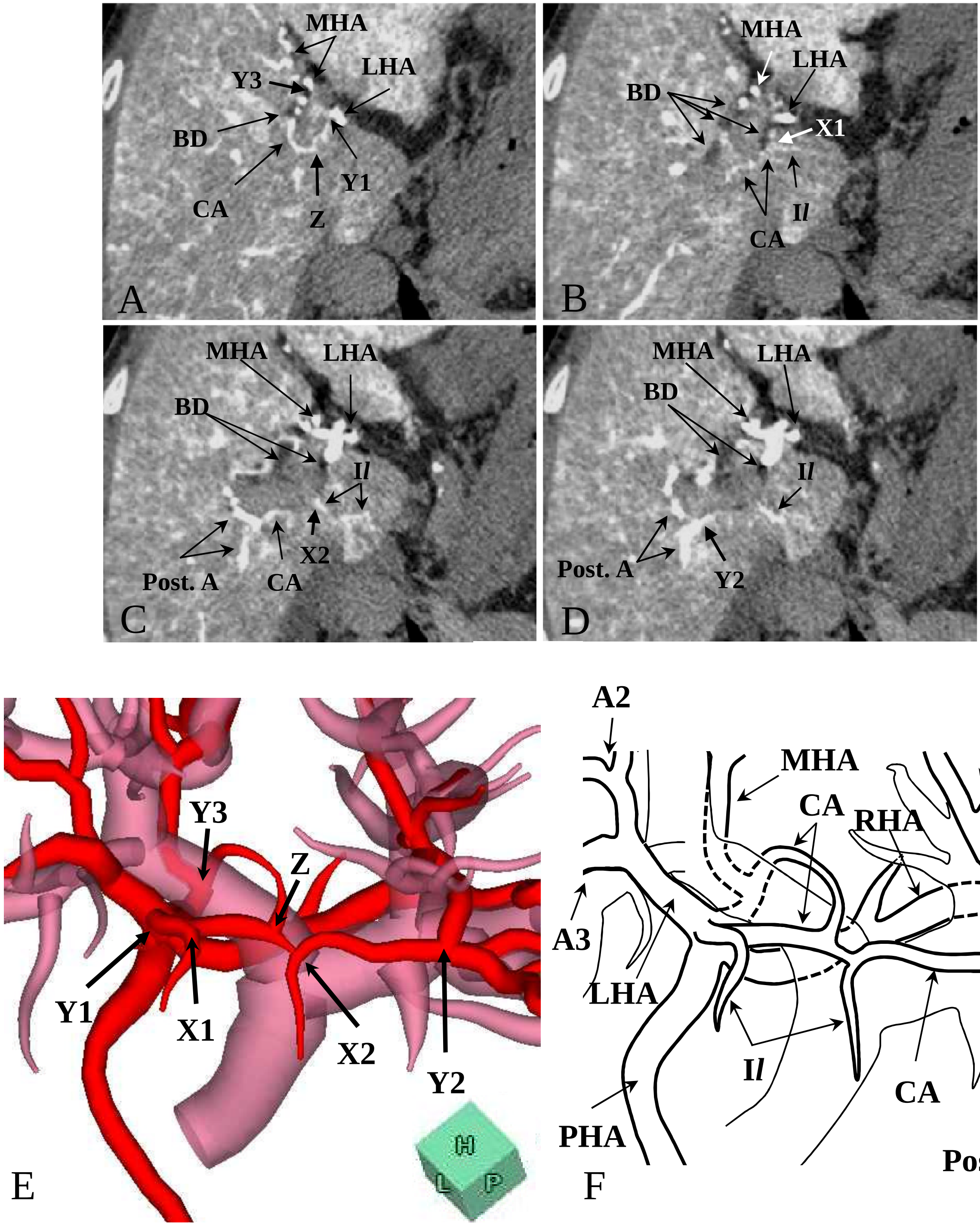

MHA
Y3
LHA
BD
Y1
CA
Z
A
MHA
LHA
BD
X1
Il
CA
B
MHA
LHA
BD
Il
X2
Post. A
CA
C
MHA
LHA
BD
Il
Post. A
Y2
D
Y3
Z
Y1
X1
X2
Y2
H
L
P
E
A2
A8
MHA
CA
RHA
A5
A7
A3
LHA
Il
CA
A6
PHA
Post. A
F

Fig. 5

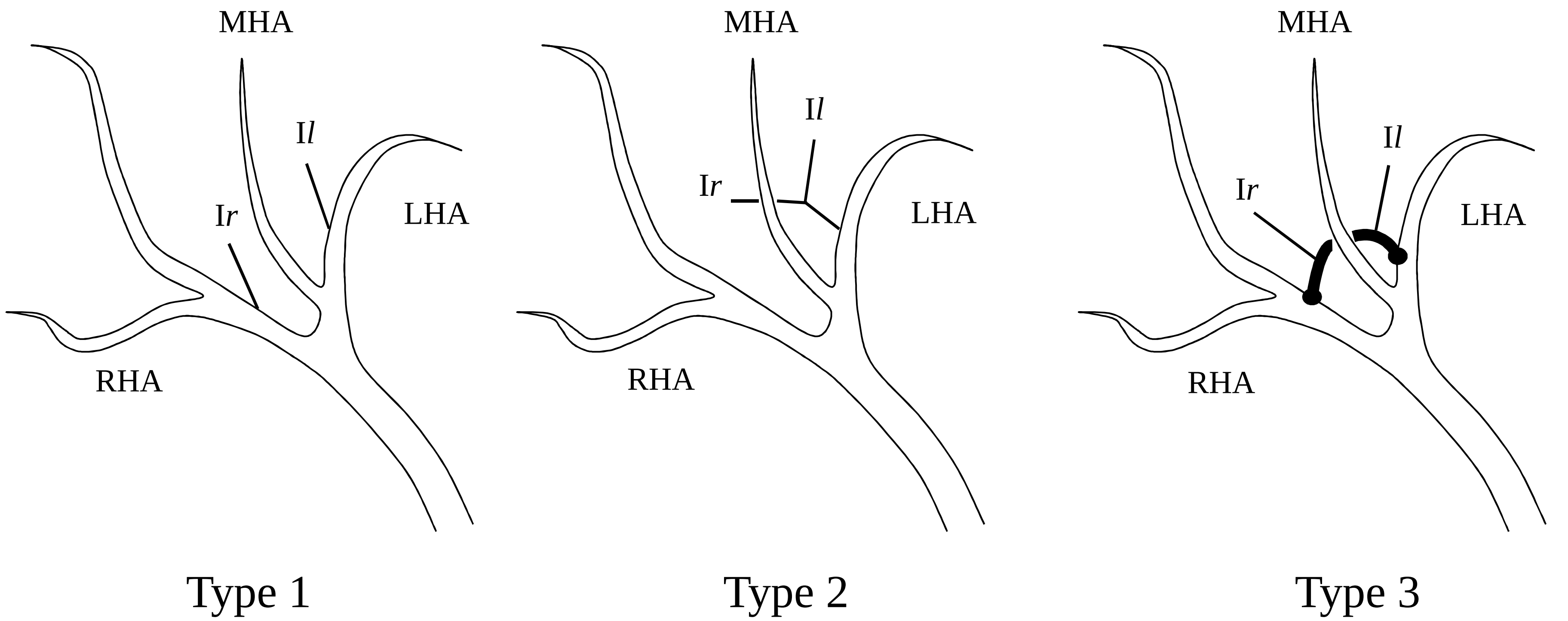
MHA
Il
Ir
LHA
RHA
Type 1
MHA
Il
Ir
LHA
RHA
Type 2
MHA
Il
Ir
LHA
RHA
Type 3

Fig. 1

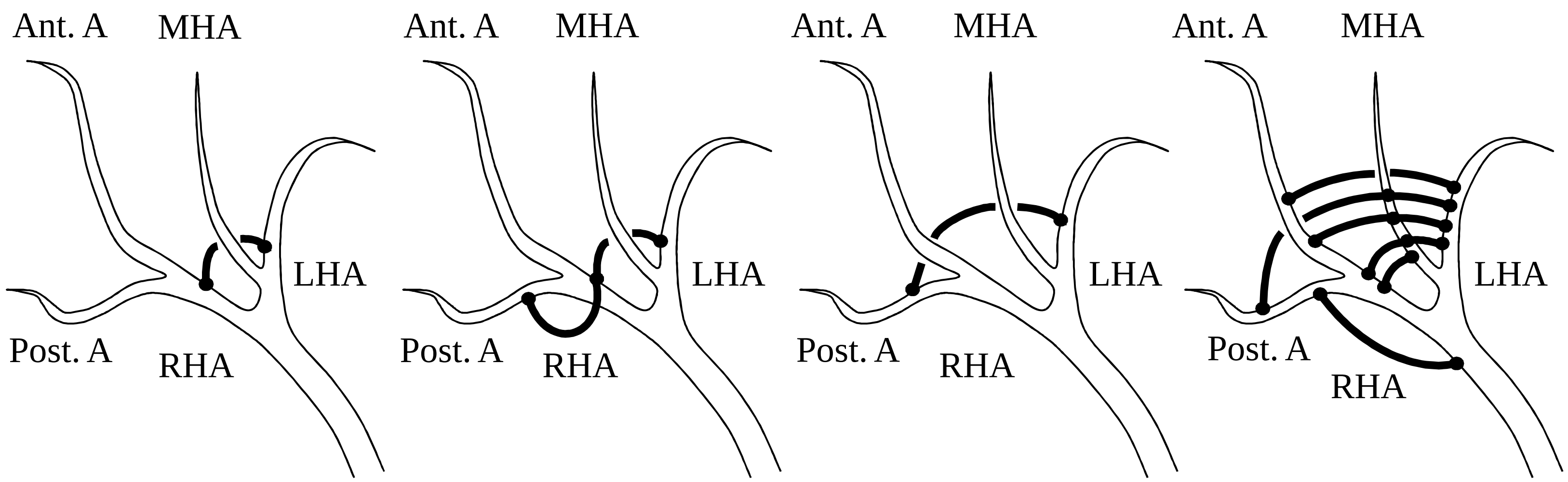

Group 1
RHA – LHA
9 (35%)

Group 2
Post. A – RHA – LHA
3 (12%)

Group 3
Post. A – LHA
3 (12%)

Group 4
Other
11 (42%)

Fig. 2

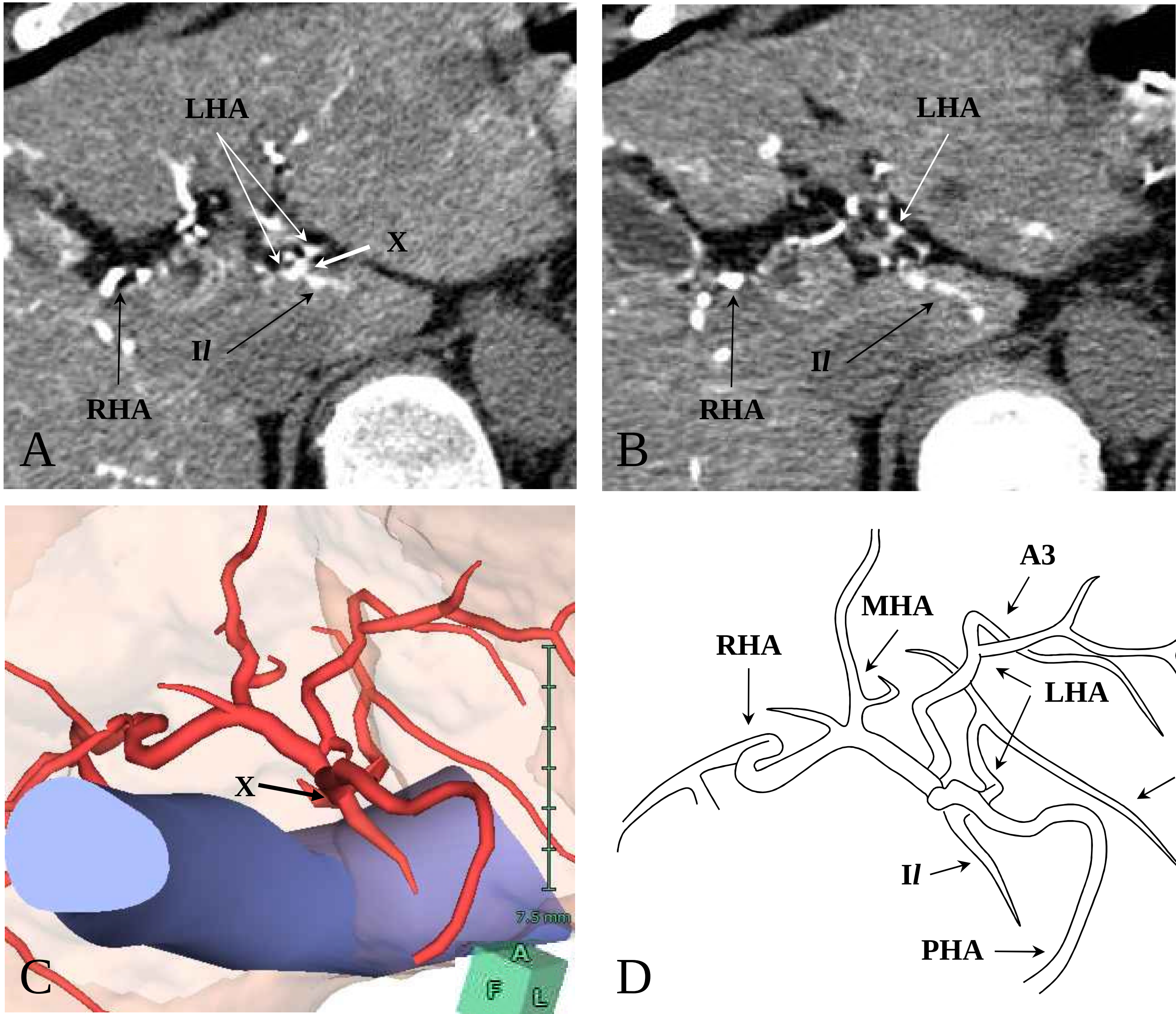

Fig. 3

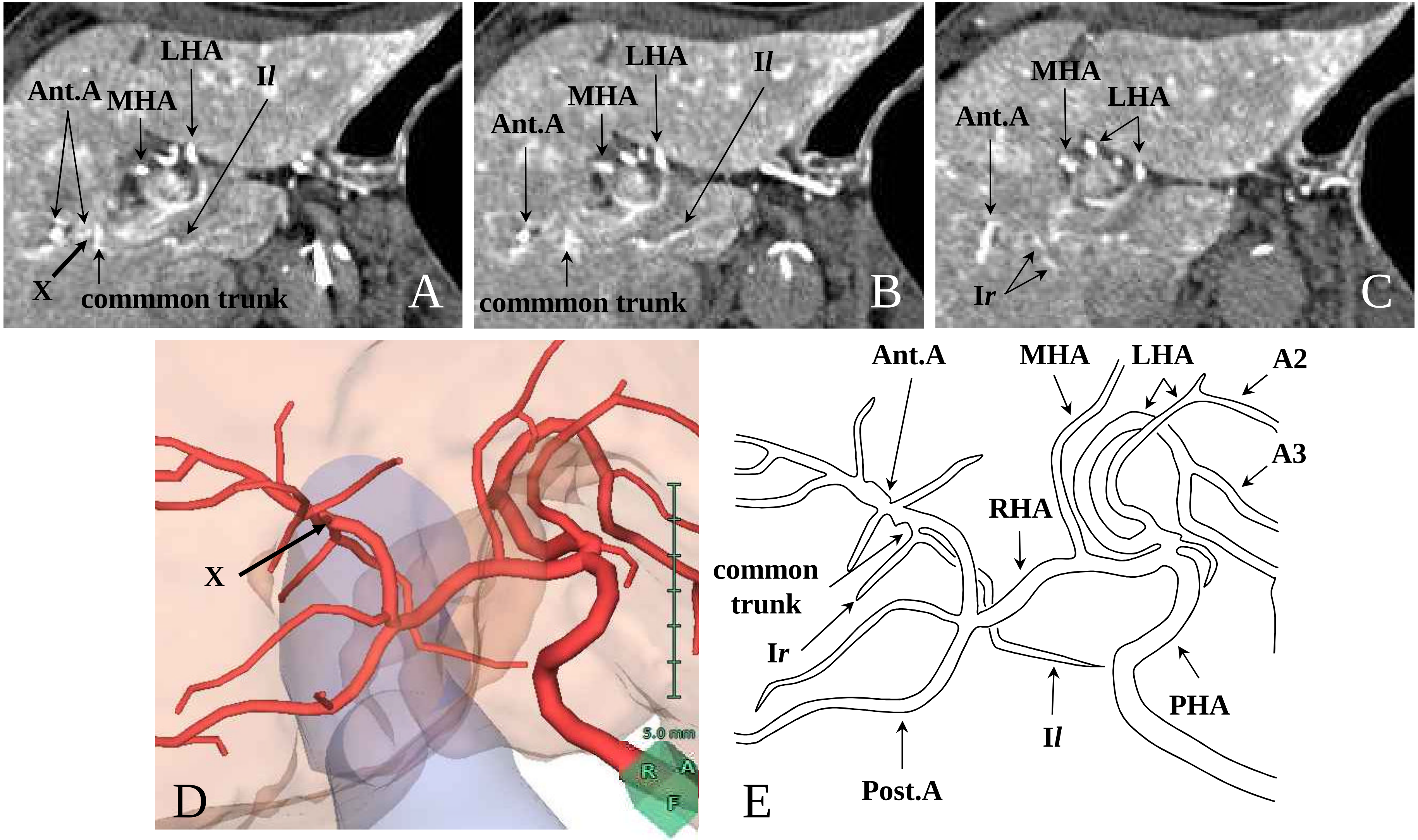

Ant.A
MHA
LHA
Il
X
commmon trunk
A
Ant.A
MHA
LHA
Il
commmon trunk
B
MHA
Ant.A
LHA
Ir
C
X
5.0 mm
D
Ant.A
MHA
LHA
A2
A3
RHA
common
trunk
Ir
Il
PHA
Post.A
E

Fig. 4